Chapter 1

Introduction

Our mathematical abilities are not strong enough to provide a theoretical understanding of many-particle systems. Statistical mechanics rescue us from finding simplified microscopic models to address many exciting features of macroscopic systems, and provides a bridge between the macroscopic thermodynamics properties and their microscopic origin [Boltzmann (1964)]. To describe a system, we need some details, i.e., shape and size of the constituent particles and their composition in the system, etc. Unfortunately, much information would be confusing. Therefore, it is worth describing a qualitative way to find the microscopic model that can explain the origin of these behaviors observed in isolated macroscopic systems, both in equilibrium and out of it. These behaviors occur for an overwhelming majority of the microstates in the micro-canonical ensemble for equilibrium-macroscopic systems. The fraction of systems with significant fluctuations from the average behavior, computed in such an ensemble, is tiny in the system's number of degrees of freedom [LEBOWITZ (2021)]. This statement is also valid for the micro-canonical ensemble subsets, describing systems in nonequilibrium macrostates. A nonequilibrium system evolve towards the equilibrium limit via time asymmetric approach, encoded in the second law and observed in individual

macroscopic systems. Once we accept the applicability of these measures to physical systems, the observed behavior does not require explanations based on ergodicity, time-averaging, or subjective information theory.

1.1 Classical systems and the thermodynamic averages

In classical mechanics, the microstate of a system is defined by a point X in a $2dN$-dimensional phase space, where N is the number of particles, i.e, $X = (\mathbf{r_1}, \mathbf{p_1}, ..., \mathbf{r_N}, \mathbf{p_N}), \mathbf{r_i} \in V \subset R^d, \mathbf{p_i} \in R^d$ [Bhattacharyajee (2000); Pathria (1996)]. And the time evolution of X is given by a Hamiltonian $H(X)$ which converges energy such that $X(t)$ is confined in a thin shell (Γ_E) surrounding the energy surface $H(X) = E$. And, we call the system to be macroscopic if $N = \mathscr{O}(10^{20})$.

We define $\rho(\mathbf{r_i}, \mathbf{p_i})$ as the probability distribution function analogous to $f(\mathbf{r_i}, \mathbf{v_i})$, where $(\mathbf{r_i}, \mathbf{p_i})$ are the phase points in a 6N-dimensional phase space volume dV. The average (or ensemble average) of a physical quantity F can be given by $\langle F \rangle = \int F \rho dV$. Another way to calculate the average of a quantity is the "time average" defined as $\bar{F} = \lim_{T\to\infty} \frac{1}{T} \int_0^T F(t)dt$. In equilibrium statistical mechanics, an event is "ergodic" if both averaging discussed above are equivalent. Other hypotheses of equilibrium statistical mechanics are the Boltzmann hypothesis discussed before and the “principle of apriori: that all the microstates, defined for a macrostate, are equally probable".

There has been significant progress in understanding different physical phenomena like collective behavior in various biological and cellular systems, etc. [Bruce Alberts & Walter (Bruce Alberts & Walter); Ma (2001); Stanley (1972)]. These systems do not follow the usual formalism of equilibrium statistical mechanics, known as the nonequilibrium system. Understanding the broad range of nonequilibrium phenomena in terms of their statistical and

thermodynamic framework is an emerging area of current research. Further, there exist many problems where particles move in an inhomogeneous environment and the interaction among particles can be ignored, e.g., transport of protein molecule through the pores of cells, the motion of electrons through a lattice, etc. Such problems can be addressed using the Lorentz lattice gas model, where particles move along the lattice bonds without any interaction. We divide this thesis into two parts; the first part covers active matter, where particles are self motile and interact via some fixed interaction rule, Sec. 1.2. In contrast, the second part addresses the problem of the Lorentz lattice gas, where particles are noninteracting, Sec. 1.9.

1.2 Active Matter: an out of equilibrium system

There can be a wide range of nonequilibrium systems showing different phenomenologies. It can be categorized based on some properties that can be common in all nonequilibrium systems. The first class can be those systems that relax toward but have not yet reached thermal equilibrium. This relaxation can be infinitely slow, e.g., relaxation of glasses. Nonetheless, there can be a specific direction towards which the system tries to move, provided the availability of sufficient energy and time. The second class consists of nonequilibrium systems whose bulk dynamics prevent them from attaining an equilibrium state due to a non-zero steady current, e.g., heat flow experiments where a matter is placed between multiple reservoirs at different temperatures. The Third class of nonequilibrium systems includes the living or *active* objects. For example, systems ranging from micron size, e.g., bacteria, biological cells, ingredients inside a cell, etc., to macrosize organisms like the animal herd, fish school, birds flock, etc. Few things are prevalent in both the class of organisms, i.e., they get the energy from their surroundings in the form of nutrients and move from one place to another. Also, they often move in the collection. The underlying physics behind this behavior is not as simple

as it is for a system in equilibrium. It is complicated to track the amount of energy consumed and converted to kinetic energy for the motion and collision in an active system. Therefore, we cannot use the physics of the equilibrium system or the time-independent energy function (Hamiltonian) to study the properties of such systems [Chaikin & Lubensky (1995); Huang (1987); Pathria (1996)]. Hence, we need a separate branch of physics to study such systems. *Active matter* is a sub-branch of nonequilibrium statistical mechanics, which provides us tools to study the physics of such systems [Dombrowski et al. (2004); Parrish & Hamner (2015); Peruani et al. (2012); Rafaï et al. (2010); Sumino et al. (2012); Surrey et al. (2001); Szabó et al. (2006)]. A particle or an agent can be termed as 'active' if it has an inherent property to take the energy from its surroundings and convert it to kinetic energy to the collective motion and collision—examples: fishes, birds, bacteria, the motor protein inside a cell, etc. We also call such 'active' objects as *self-propelled particles (SPPs)*. A system composed of SPPs is called an active system or active matter [Cates (2012); Marchetti et al. (2013); Ramaswamy (2010, 2017); Toner et al. (2005); Vicsek & Zafeiris (2012); Yates et al. (2011)]. We can name almost every *living* organism as "Active matter"; further, there can be artificial systems, e.g., active colloids [Bricard et al. (2013); Cates & Tailleur (2015); Theurkauff et al. (2012)], active polar disks [Deseigne et al. (2010)], vibrated rods [Blair et al. (2003); Kumar et al. (2014); Narayan et al. (2006); Narayan et al. (2007)], etc., that can fall into the category of active matter.

Further, the active systems are not similar to the other out of equilibrium systems, e.g., bulk fluid sheared from the top, the driven diffusive systems, etc. However, we can define a nonequilibrium steady state (NESS) similar to other out-of-equilibrium systems. We define the nonequilibrium steady state when the relevant macroscopic observables remain statistically the same for a long time. In contrast, in the equilibrium steady-state, the observed macrostates remain unchanged with time. For example, NESS is achieved in a fish school or a bird flock

when all the agents (fish/bird) move coherently. Therefore, we can consider this flocking arrangement as a steady-state with a non-zero steady particle current.

If $P(X,t)$ is the probability of finding the system in a microscopic configuration X at time t. The time evolution of $P(X,t)$ is defined by the Master equation,

$$\frac{d}{dt}P(X,t) = \sum_{X' \neq X} [W(X' \to X)P(X',t) - W(X \to X')P(X,t)], \tag{1.1}$$

where $W(X' \to X)$ is the transition rate from configuration X' to X. In the equilibrium steady-state, $P(X,t)$ is no longer function of time; hence the left hand side of the Eq. (1.1) will vanish. Therefore, the probability of the system going from configuration X to X' is the same as the probability of the system going from X' to X. Hence, the *detail balance* is satisfied in an equilibrium system. But, in the case of an active system, there is a net steady state non-zero energy current in the system, hence the detailed balance violation. In some cases of active matter, an "effective temperature" can be defined in a certain limit of associated parameters. Hence, an effective fluctuation-dissipation-relation (FDR) can be defined [Fodor et al. (2016); Loi et al. (2008); Speck (2016); Speck et al. (2014); Szamel (2014); Tailleur & Cates (2008)].

Another important feature of active systems is that they show large density fluctuation compared to the equilibrium counterparts in the steady state. In real space, if a region of volume V contains N number of particles on average, the system ordinarily shows fluctuations with standard deviation $\Delta N \propto \sqrt{N}$ provided that the system is not close to a critical point. In the active matter systems, the density fluctuations grow faster than as $\sqrt{N}$, and in two dimensions, it also grows as fast as N in some cases [Ramaswamy et al. (2003); Toner et al. (2005)].

1.3 Details of Active matter

Active particles, in general, are elongated in shape, and their direction of motion is decided by their anisotropy rather than in the direction of some fixed external field. Therefore the orientational order is one of the key features in the active matter system, e.g., the swarm of myxobacteria [Copenhagen et al. (2021); R. Kemkemer & Gruler (2000)], fish school [Toner & Tu (1995); Vicsek et al. (1995a)], etc. The natural systems ranges from micro size, e.g., bacteria [Copenhagen et al. (2021)], in vitro mixture of cell extracts of biofilaments and associated molecular motor proteins [Doostmohammadi et al. (2016b)], etc., to macro size systems like the animal herd, fish school [Vicsek et al. (1995a)], birds flock [Toner & Tu (1995)], etc. A non-living active system can arise by vibrated rods [Narayan et al. (2006); Narayan et al. (2007)], colloidal and the nanoscale particle, which is propelled through a fluid by the surface chemistry of the particles and the underlying medium, and swarming drones. Indeed, the active systems are distinct from the other nonequilibrium systems in terms of the energy input, i.e., the energy input in the active system is local (at single-particle level), not at the boundary of the surface, e.g., shear flow in the bulk fluid. Each active particle goes through a cycle of energy exchange, where it takes and dissipated energy, which fuels the internal changes and results in the collective motion. Active systems exhibit many exciting nonequilibrium properties, including emergent structures in the collective motion, which is absent at the single-particle level, large density fluctuation, nonequilibrium order-disorder transition, pattern formation on mesoscopic scales, unusual mechanical and rheological properties [Aditi Simha & Ramaswamy (2002); Cates et al. (2008); Giomi et al. (2010); Mishra & Ramaswamy (2006)], etc.

Living systems are the best outstanding example of active systems. They exhibit extraordinary properties such as spontaneous motion and dynamical organization; they also include generating and responding in a calibrated manner to forces. Due to immense system

complexity, a theoretical description to explain all the general properties of an active system is very difficult to achieve; for example, the complexity inside a cell makes it very difficult to provide a theoretical description to address all the phenomenology altogether.

Therefore, understanding a living organism's complex dynamical behavior is one of the main motivations to prepare a simple theoretical description for active systems. Also, it has been found that the active system shows long-wavelength behavior [Manneville et al. (2001); Prost & Bruinsma (1996); Ramaswamy & Rao (2001); Ramaswamy et al. (2000)]. The general theoretical description to address the flocking behavior of active agents in bulk, e.g., fish school, birds flock, animal herds, is provided in [Toner & Tu (1995, 1998); Toner et al. (2005)]. Further, the macroscopic mechanical properties of cytoskeletal filaments as an active gel are described in [Jülicher et al. (2007); K. Kruse (2005)].

There can be several methods to study the phenomenological behavior of active systems. The agent-based description is one of them and is widely used. The agent-based (or rule-based) model, first given in 1995 by Vicsek and coworkers [Vicsek et al. (1995b)], mainly emphasizes macroscopic properties' fluctuation rather than forces and mechanics. In this model, flocking is addressed as the phase transition from disorder to order. Further, the modification and variant of the Vicsek model came from time to time [Chaté et al. (2006, 2008); Grégoire & Chaté (2004)]. These models, in general, takes the agents in the system as point-like particles with a fixed speed in an inert environmental background where the particle to particle interaction and thermal noise govern the direction of particles' motion. A particle aligns itself according to the orientation of its neighbors. This family of theoretical models successfully displayed the well-defined order-disorder transition for different amounts of noises in the system or increasing particle densities.

The results, which focus on the large-scale generic behavior, are mainly obtained from the computer-based numerical simulation. In active systems, many macroscopic properties

are universal irrespective of their length scale. They operate and significantly differ in their dynamics at the microscopic level; for example, the flocking phenomena are visible in the fish school [Parrish & Hamner (1997)], and collections of melanocyte cells [R. Kemkemer & Gruler (2000)]. Another example is the contractile stress, which is evident at the subcellular level [Joanny & Prost (2009); Poul M. Bendix (2008)] and in a large collection of cells swimming in algae [Rafaï et al. (2010)].

1.4 Categories of active matter systems

Active matter can be divided into a number of classes based on symmetry and conservation laws with well defined collective behavior. Active system can be divided into four classes basses on the shape and symmetry and the momentum conservation law.

1.4.1 Polar and Apolar active matter

According to the nature of the broken symmetry of the ordered phase, the active objects are of two types: polar and apolar objects. Polar entities have distinct heads and tails, e.g., fish school, birds flock, animal herds, etc. Polar objects can order in a polar fashion with all the active particles oriented in their heading direction, with a non-zero magnetization, or order in a nematic phase with zero magnetization. Apolar objects do not distinguish between head and tail, e.g., melanocyte cells. Apolar objects form the ordered phase only with nematic order. An schematic diagram of polar and apolar particles and their ordering phases are shown in fig. 1.1.

A vector can describe polar objects with the arrow pointing in the direction of the head, and the ordered state is characterized by a vector order parameter **P**. As the nematic

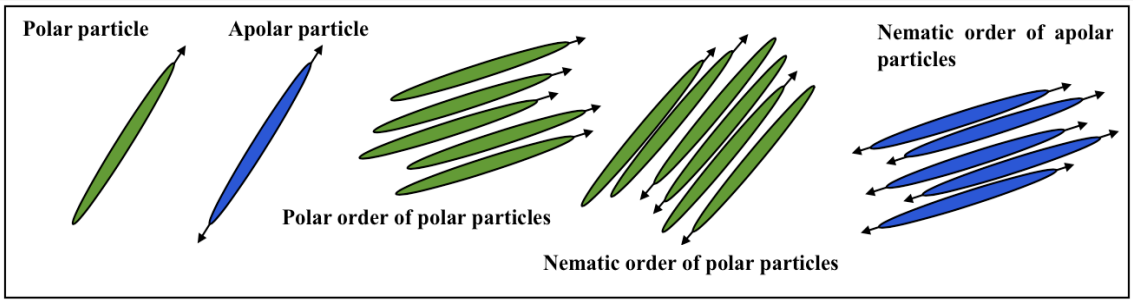

Fig. 1.1 Schematic diagram of polar and apolar partiles and their ordering states. Arrow shows the direction of motion, double arrow represents the head and tail symmetry.

order is symmetric along the elongated axis of the object, a vector cannot define the nematic order. Therefore a tensor, $\mathscr{Q}$, is used to describe the nematic order parameter, called as alignment tensor. The difference between the polar order can be visible in the *in vitro* sample of kinesin motor protein [Surrey et al. (2001)]. In contrast, the nematic order can be seen in the melanocyte cells forming the topological defects [R. Kemkemer & Gruler (2000)].

1.4.2 Dry and Wet active matter

We refer to a system as dry when the system violets the momentum conservation. These systems include the motion of bacteria on a rigid surface [Wolgemuth (2002)], animal herds [Toner & Tu (1998)], birds flock [Ballerini et al. (2008); Ginelli & Chaté (2010)], vibrated granular rods on a substrate [Aranson & Tsimring (2006); Deseigne et al. (2010); Kudrolli et al. (2008); Narayan et al. (2007); Ramaswamy et al. (2003); Yamada et al. (2003)]; in all these systems, the momentum is damped by the friction between the active particles and the underlying substrate. Further, the motor filament suspension [Liverpool (2003)], and a concentrated collection of swimming bacteria [Drescher et al. (2011)] can also be considered dry as the steric hindrance, and thermal fluctuation suppresses the hydrodynamic interactions. In a dry system, the only conserved quantity is the number of particles (neglecting the death and reproduction), and the hydrodynamic fields are the local density and orientation order

parameter since both are non-zero in the broken symmetry state. In contrast, when the active objects are suspended in a fluid, and the interaction between the particles and the fluid cannot be neglected, such systems are called “wet”. In a wet system, momentum conservation is strictly followed.

There are several studies that address the “dry” and “wet” systems categorically discussing the polar and apolar systems. Example: it dry polar system - animal herds [Parrish & Hamner (1997)], cell layers [Xavier Serra-Picamal & Trepat (2012)], vibrated asymmetric granular particles [Kudrolli et al. (2008)], films of cytoskeletal extracts [Surrey et al. (2001)]; *dry nematic systems* - melanocyte cells on a plastic surface [R. Kemkemer & Gruler (2000)], vibrated granular rods [Narayan et al. (2007)]; *wet polar system* - cell cytoskeleton and cytoskeletal extracts in bulk suspensions [Poul M. Bendix (2008)], swimming bacteria in bulk [Dombrowski et al. (2004)], Pt catalytic colloids [Palacci et al. (2010)]; *wet nematic systems* - suspension of microtubules and motor proteins in oil [Doostmohammadi et al. (2016a)], colonies of m. xanthus bacteria [Copenhagen et al. (2021)], suspensions of catalytic colloidal rods [Paxton (2004)], etc.

1.5 Methods to study active matter

We can study the active matter system generally in three ways; by solving (1) agent based equations of motion, (2) hydrodynamic equations of motion written for the coarse grained hydrodynamics variables, e.g., density and order parameter fields and (3) using experimental techniques. Now we discuss some of the methods to study overdamped active matter systems in the following subsections:

1.5.1 Agent based models: Vicsek Model

Agent-based models are again of two types; first, microscopic rule-based model, e.g., Vicsek model [Vicsek et al. (1995b)], and second, Langevin's equation of motion. Vicsek model (VM) describes a rule-based model for the movement of polar particles (fish school and bird flocks). In VM, each self-propelled particle interacts with its neighboring particles with a fixed rule within an interaction radius. Further, the velocity direction of the polar particles is dictated by some angular noise—the polar order forms via head-to-head alignment of particles and form large ordered domains. Furthermore, the Vicsek model can also be extended for apolar particles. The update equations in Vicsek model are,

$$\mathbf{r}_i(t+1) = \mathbf{r}_i(t) + \mathbf{v}_i \Delta t, \tag{1.2}$$

is the position update equation and,

$$\theta_i(t+1) = \langle \theta(t) \rangle_{\mathscr{R}} + \eta \Delta\theta \tag{1.3}$$

is the orientation update equation for the i^{th} particle. Here, $\mathbf{r}_i$, $\mathbf{v}_i$ and θ_i are the position, the self-propulsion speed and the orientation of the i^{th} particle. $\langle \theta(t) \rangle_{\mathscr{R}}$ is the mean orientation of the particles within an interaction radius $\mathscr{R}$. Δt (fixed) is the step-size for the update in time. $\Delta\theta \in (-\pi, \pi)$ is the random noise in the alignment and $\eta \in [0,1]$ is the noise strength. The second term in eq. 1.3 is called the "angular noise" as it applies to each particle such that it rotates by some small angle from its original direction.

Density ρ, which is the number of particles per unit area, and the noise strength η are the two control parameters in the VM. Numerical simulation of Eqs. 1.2 and 1.3 show that

the system shows a continuous phase transition from a disordered state to the ordered state by changing the noise from high to low. Different exponents are observed near the phase transition as in the equilibrium counterparts. In more detail, the collective motion of particles in the different limits of η and ρ, show three distinct regimes; (i) for small ρ and η, the particles tend to form groups moving coherently in random directions, (ii) at higher densities and noise the particles move randomly with some correlation, and (iii) for higher density and small noise the motion becomes ordered.

Further, the noise in the VM can be either angular (scalar) or vector. To address the nature of order-disorder transition in polar SPPs, chaté and the co-workers introduced "vector noise" [Chaté et al. (2007, 2008); Grégoire & Chaté (2004)], described by the update equation for the position given in Eq. 1.2 and the update for orientation is provided by,

$$\theta_i(t+1) = Arg[\sum_{k\sim i} e^{i\theta_k(t)} + \eta n_i(t) e^{i\phi_i(t)}], \tag{1.4}$$

In two dimensions, $Arg = tan^{-1}(y/x)$ where x and y are the poistion of the particles from the origin. Here, $n_i(t)$ is the number of particles in the neighbour to i^{th} particles within the interaction range at any time t. ϕ_i is the random angle $\in (0, \pi)$. Further, for angular noise, the nature of the order-disorder transition becomes discontinuous provided one considers significant enough system size. Hence, the finite size effect is much more dominant for angular noise [Vicsek et al. (1995b)] compared to the vector noise choice [Ai et al. (2013)]. The nature of the phase transition in these systems is still a problem of interest. In various studies, the nature of the transition depends on the system's update mechanism [Aldana et al. (2007)]. It is observed that the density phase separation is the key to making the transition first-order [Pattanayak & Mishra (2018); Solon et al. (2015)]. But there is still a lack of experiments to answer this question in natural systems.

1.5.2 Agent based model : Langevin's dynamics

There is another class of particles, and it is pretty hard to place them in the category of polar/apolar objects. Granular particles and colloidal suspension are examples, often called active Brownian particles(ABPs). ABPs, unlike the asymmetric polar/apolar particles, are symmetric in shapes like a disk or a sphere. The term "Brownian" comes because these particles move in an environment with thermal fluctuation similar to the passive Brownian particles. Being active by nature, they perform a "persistent random walk" rather than the usual random walk. Langevin's equation of motion, traditionally used for studying equilibrium granular particles, can also be used to study active Brownian particles. We add one more term to describe an active system to Langevin's equation called the "active" term or the "activity". Langevin's equation of motion for a position update is given as,

$$\frac{\partial}{\partial t}\mathbf{r}_i(t) = v_0\hat{\mathbf{e}}_i + \mu\sum_j^N \mathbf{F}_{ij} + \sqrt{2D_T}\eta_i^T(t), \tag{1.5}$$

and for the orientation update,

$$\frac{\partial}{\partial t}\theta_i(t) = \sqrt{2D_R}\eta_i^R(t) \tag{1.6}$$

On the left-hand side of Eq. (1.5), the inertial term is omitted, and it doesn't change the qualitative result much for a dense system (or low Reynolds number). In Eqs. (1.5) and (1.6), $\mathbf{r}_i(t)$ is the position of i^{th} particle at time t, v_0 is the self-propulsion speed which is same for all the particles and, $\theta_i(t)$ is the orientation angle which defines $\hat{\mathbf{e}} = (cos(\theta), sin(\theta))$. The interaction force between the particles is, $\mathbf{F}_{ij} = -\nabla U(r_{ij})$, where $U(r_{ij})$ is the pair interaction potential between the particles, $r_{ij} = |\mathbf{r_i} - \mathbf{r_j}|$ is the separation between two particles. μ is the

mobility and is inversely proportional to the friction coefficient such that each particle is driven by a constant force of magnitude equal to $\frac{v_0}{\mu}$. $(\mu\kappa)^{-1}$ is the elastic time scale. η is the random Gaussian white noise with mean zero, $\langle\eta(\mathbf{r},t)\rangle = 0$ and $\langle\eta(\mathbf{r},t)\eta(\mathbf{r}',t')\rangle = \delta(\mathbf{r}-\mathbf{r}')\delta(t-t')$, here D_T and D_R are the translational and rotational diffusion coefficient respectively. D_R^{-1} is the time scale over which the orientation of the active particle changes. Hence, $l_p = v_0 D_R^{-1}$, the persistence length or the run length, is the typical distance travelled by an active particle before it changes direction.

Active Brownian particles show motility-induced phase separation (MIPS) even at a very low particle density using Langevin's dynamics described above [Cates & Tailleur (2015); Levis & Berthier (2014); Redner et al. (2013); Stenhammar et al. (2013); Tailleur & Cates (2008)]. Langevin's dynamics can also be used to study the effect of polydispersity on the dynamics of active Brownian particles Kumar et al. (2021), jamming in a tissue Bi et al. (2016), etc.

1.5.3 Hydrodynamics equations of motion

The previous method of agent-based approach to describe and study the active matter is based on the microscopic details of the system. In the generalized hydrodynamic approach, we write the equation for slow variables *viz.* density and orientation fields in a coarse-grained description of large scale and long time behavior. The time evolution of this variable is written in terms of the continuum or hydrodynamic equations following the liquid crystal hydrodynamics in [Martin et al. (1972); de Gennes & Prost (1993)], with additional nonequilibrium terms due to activity in the system. The convenience of using generalized hydrodynamic theories is due to the fact it successfully describes the many condensed matter systems, e.g., superfluids [Dzyaloshinskii & Volovick (1980)], liquid crystals [Martin et al. (1972)], polymers [Milner (1993)], as well as simple fluids. One way to obtain the hydrodynamic description for the active system is based on the microscopic models and using the tools of statistical mechanics

to coarse-grained the model for long-wavelength and long-timescale equations [Ahmadi et al. (2005, 2006); Aranson & Tsimring (2005); Kruse & Jülicher (2003); Liverpool (2003)]. Another way to obtain the hydrodynamic theory is to directly write hydrodynamic equations for microscopic fields, including all terms allowed by the symmetry as Toner and Tu [Toner & Tu (1995, 1998)] did for the dry flocks. Further, this approach can be extended for the suspension of SPPs in a fluid [Aditi Simha & Ramaswamy (2002)] and active filaments solution [Hatwalne et al. (2004)].

Here, we write the hydrodynamic equation for the motion for dry active systems. The only conserved quantity, in this case, is the number of particles in the system, neglecting the death and rebirth, and the associated hydrodynamic field is the local density of the active units. The ordering of polar and apolar particles is described below. The self-propelled units in the first-class form polar order as described in the classic Vicsek model [Vicsek et al. (1995b)]. The second class forms nematic order either with apolar units, e.g., melanocytes [Gruler, H. et al. (1999)] or polar, such as self-propelled hard rods [Baskaran & Marchetti (2008); Peruani et al. (2006); Yang et al. (2010)]. A cartoon of the different cases is shown in Fig. 1.1.

The Vicsek model describes the motion of self-propelled polar particles with fixed speed and noisy interaction, which shows the nonequilibrium disorder-order phase transition for high density and low noise. Toner and Tu have proposed a phenomenological continuum model, based on the symmetry considerations, inspired by the Vicsek model. Further, a coarse-grained approach was adopted to derive the Toner and Tu continuum model from the microscopic rule based Vicsek models, as in [Bertin et al. (2006, 2009); Ihle (2011)]. These derivations provided a microscopic basis for the hydrodynamic theory. For a collection of self-propelled particles moving on a frictional substrate, the only conserved quantity is the density $\rho(\mathbf{r},t)$ of the active particles. For polar particles, the polar order is defined by the polarization vector field $\mathbf{p}(\mathbf{r},t)$, also called the polar order parameter. These continuum fields can be defined in

terms of position vector $\mathbf{r}(t)$ and the unit vector $\hat{v}(\mathbf{r},t)$ where, $\hat{v} = (cos\theta(\mathbf{r},t), sin\theta(\mathbf{r},t))$ in two dimensions, as,

$$\rho(\mathbf{r},t) = \sum_n \delta(\mathbf{r} - \mathbf{r}_n(t)) \tag{1.7}$$

$$\mathbf{p}(\mathbf{r},t) = \frac{1}{\rho(\mathbf{r},t)} \sum_n \hat{v}(\mathbf{r},t)\delta(\mathbf{r} - \mathbf{r}_n(t)) \tag{1.8}$$

and the hydrodynamic equations of motion are given as,

$$\partial_t \rho + v_0 \nabla \cdot (\rho \mathbf{p}) = -\nabla \cdot (-\frac{1}{\gamma_\rho} \nabla \frac{\delta F_p}{\delta \rho} + \mathbf{f}_\rho) \tag{1.9}$$

$$\partial_t \mathbf{p} + \lambda_1 (\mathbf{p} \cdot \nabla)\mathbf{p} = \frac{1}{\gamma} \frac{\delta F_p}{\delta \mathbf{p}} + \mathbf{f}(\mathbf{r},t), \tag{1.10}$$

where, v_0 is the self-propulsion speed of the individual active particle, γ_ρ and γ are the kinetic coefficients. F_ρ is the free energy functional given as,

$$F_{\mathbf{p},\rho} = \int_{\mathbf{r}} \{ \frac{\alpha_1(\rho)}{2} |\mathbf{p}|^2 + \frac{\beta_1}{4} |\mathbf{p}|^4 + \frac{\kappa}{2} (\partial_i p_j)(\partial_i p_j) + \frac{\omega}{2} |\mathbf{p}|^2 \nabla \cdot \mathbf{p} - \omega_1 \nabla \cdot \mathbf{p} \frac{\delta \rho}{\rho_0} + \frac{A}{2} (\frac{\delta \rho}{\rho_0})^2 \}, \tag{1.11}$$

The first term on the right hand side of Eq. (1.9) is the diffusive term and $\mathbf{f}_\rho$ is the associated noise. λ_1 is the controls the advective term on the left hand side of Eq. (1.10). Further these equations are not Galilean invariant which requires $\lambda_1 = v_0$. Therefore, λ_1 is a non-universal phenomenological parameter determined from the microscopic properties. According to Toner -Tu continuum model, $\mathbf{p}(\mathbf{r},t)$ acts as orientational order parameter in the system as well as particles velocity current $v_0\mathbf{p}$. Also, it acts on itself by flow alignment and advection, which contributes to the $(\mathbf{p}\cdot\nabla)\mathbf{p}$ in the $\mathbf{p}$ equation. Whereas, in the density equation, $\mathbf{p}$ appears with a velocity like character only. Also, the condition $\lambda_1 \neq v_0$ provides the fluctuation in the density and polarization that can be convected at different speeds. Finally, the last term on the right-hand side of Eq. (1.10) is the purely additive Gaussian white noise with zero mean and correlation, $\langle f_i(\mathbf{r},t) f_j(\mathbf{r}^{'},t^{'})\rangle = 2\Delta\delta_{ij}(\mathbf{r}-\mathbf{r}^{'})\delta(t-t^{'})$ where i,j are the space indices in two dimensions, that takes care of the fluctuations in the system. In Eq. (1.11), ρ_0 is the average density and $\delta\rho = \rho - \rho_0$ is the fluctuation in the density about its mean value ρ_0. Such fluctuation results a compression in the system with modulus A. Further, the first two terms in Eq. (1.11) are the mean field terms for continuous order-disorder transition when α_1 changes sign. α_1 depends on the density and the noise in the system and becomes negative at or above the critical density (ρ_c). It can be defined as $\alpha_1 = a_0(1-\rho/\rho_c)$, and a_0 controls the rate of rotational diffusion as $D_r = a_0/\gamma$. For a stable system, $\beta_1 > 0$. The third term is the Frank energy term for the elastic deformations in the system, with κ as the Frank constant. These terms also take care of splay and bend in the order parameter [Voituriez et al. (2006a)]. Again the forth and fifth terms gives the density and $|\mathbf{p}|^2$ contribution to the splay. using equation (1.11), $\mathbf{p}(\mathbf{r},t)$ equation take the form,

$$\partial_t\mathbf{p} + \lambda_1(\mathbf{p}\cdot\nabla)\mathbf{p} = -[\alpha(\rho) + \beta|\mathbf{p}|^2]\mathbf{p} + \kappa\nabla^2\mathbf{p} - v_1\nabla\frac{\rho}{\rho_0} + \frac{\lambda}{2}\nabla|\mathbf{p}|^2 - \lambda\mathbf{p}(\nabla\cdot\mathbf{p}) + \mathbf{f}, \tag{1.12}$$

where, $v_1 = \omega_1/\gamma$ and $\lambda = \omega/\gamma$, also present in equilibrium ferromagnetic systems, have the dimensions of velocity and are the coupling between density and the local order. Quantities, $\alpha = \alpha_1/\gamma$, $\beta = \beta_1/\gamma$.

Homogeneous steady-state: The dynamical equation of motion, Eqs. (1.9) and (1.12), for a system with a collection of polar particles show ordered and disordered states under different conditions. For $\alpha > 0$ or $\rho_0 < \rho_c$, the system is in the disordered or isotropic state with $\mathbf{p} = 0$ and zero mean velocity. For $\alpha < 0$ or $\rho_0 > \rho_c$, system exhibits an ordered state with polar order parameter $|\mathbf{p}| = \sqrt{-\alpha_0/\beta}$, where $\alpha_0 = \alpha(\rho_0)$. Further, in the ordered state, the system moved with a velocity $\mathbf{v} = v_0\mathbf{p}$ and, the continuous rotational symmetry is broken. This mean-field analysis is also valid with fluctuation corrections in two dimensions [Toner & Tu (1995, 1998)], evaded the Mermin-Wagner theorem forbidding (at equilibrium) the spontaneous breaking of continuous symmetry in two dimensions [Chaikin & Lubensky (1995); Hohenberg (1967); Mermin & Wagner (1966)]. The Mermin-Wagner theorem is not valid for such a nonequilibrium system; due to the presence of advective non-linearities in equation (1.9) and (1.12). It leads to an effective long-range order in the system, even if the density fluctuation is ignored [Toner (2012)].

Properties of the isotropic state: The linear stability analysis of the homogeneous steady state can be done in terms of inhomogeneous fluctuations. Let $\delta\rho = \rho - \rho_0$ and $\delta\mathbf{p} = \mathbf{p} - \mathbf{p}_0$ are the fluctuations in the density and the order parameter from the value in the homogeneous states, ρ_0 and $\mathbf{p}_0$ as discussed in the previous section. The isotropic state is

characterized by $\rho_0 < \rho_c$ and $\mathbf{p}_0 = 0$. Therefore the equation for the dynamics of the linear fluctuation $(\delta\rho, \delta\mathbf{p})$ can be given as,

$$\partial_t \delta\rho = -v_0\rho_0\nabla\cdot\mathbf{p}, \tag{1.13}$$

$$\partial_t \mathbf{p} = -\alpha_0\mathbf{p} - \tfrac{v_1}{\rho_0}\nabla\delta\rho + \kappa\nabla^2\mathbf{p} + \mathbf{f}, \tag{1.14}$$

where $\alpha_0 > 0$. The dispersion relation in between the frequency ω and the wave vector $\mathbf{q}$ can be obtained by taking the Fourier transforms of Eqs. (1.13) and (1.14), which gives us the modes of the form $e^{(\mathbf{q}\cdot\mathbf{r}-i\omega t)}$. Polarization fluctuations transverse to $\mathbf{q}$ decouple and decay at a rate $\alpha_0 + \kappa q^2$. The relaxation of coupled fluctuations of density and longitudinal polarization is controlled by the coupled hydrodynamic modes with frequencies [Marchetti et al. (2013)],

$$\omega^I_{\pm}(q) = -\tfrac{i}{2}(\alpha_0 + \kappa q^2) \pm \tfrac{i}{2}\sqrt{(\alpha_0 + \kappa q^2)^2 - 4v_0v_1q^2} \tag{1.15}$$

For linear stability the fluctuation must decay at long time so that $Im[\omega(q)] < 0$. The isotropic state is linearly stable for all parameter values with the condition $v_0v_1 > 0$, where v_1 is like an effective compressional modulus. At a low density, the microscopic derivatives of the continuum models yields $v_1 = v_0/2$ [Baskaran & Marchetti (2008); Bertin et al. (2006, 2009); Ihle (2011)]. In this case $v_1 > 0$ and the isotropic state is always stable. At high density, however, caging effects can result in a density dependence of v_1, which can in turn lead to

a density instability of the isotropic state as shown by [Tailleur & Cates (2008)] and [Fily et al. (2012)]. In this, for a stable isotropic state the dispersion relation for $\alpha_0 \leq v_0 v_1/\kappa$ in the wavevector range $q_{c-} \leq q \leq q_{c+}$ [Baskaran & Marchetti (2008); Ramaswamy & Mazenko (1982)],

$$q_{c\pm}^2 = \frac{2v_0v_1}{\kappa^2}[1 - \frac{\kappa\alpha_0}{2v_0v_1} \pm \sqrt{1 - \frac{\kappa\alpha_0}{v_0v_1}}] \tag{1.16}$$

Density fluctuations then propagated as wave-vector instead of diffusing. Near the transition, where $\alpha_0 \to 0^+$, we find $q_{c-} \to 0$ and $q_{c+} \simeq 2\sqrt{v_0v_1}$. These propagating sound-like density waves are ubiquitous in collection of self-propelled particles [Aditi Simha & Ramaswamy (2002); Giomi et al. (2008, 2011, 2012); Kruse et al. (2004); Voituriez et al. (2005, 2006b)].

Properties of the ordered state: Now we analyse the linear stability of the ordered state by considereng linear dyanmics of fluctuations about $\rho_0 > \rho_c$ and $\mathbf{p}_0 = p_0\hat{\mathbf{x}}$. We can write $\mathbf{p} = p\hat{\mathbf{n}}$, where $\hat{\mathbf{n}}$ is the unit vector pointing in the direction of the local orientational order. Hence we have $\delta\mathbf{p} = \hat{\mathbf{n}}_0\delta p$. The condition $|\hat{\mathbf{n}}|^2$ requires that $\hat{\mathbf{n}}_0 \cdot \delta\mathbf{n} = 0$. For two dimensional coordinate system, $\hat{\mathbf{n}}_0 = \hat{\mathbf{x}}$ and $\mathbf{n} = \delta n\hat{\mathbf{y}}$ and $\mathbf{p} = \hat{\mathbf{x}}\delta p + \hat{\mathbf{y}}p_0\delta n$. The linearized equations as given in [Marchetti et al. (2013)], are,

$$(\partial_t + v_0p_0\partial_x)\delta\rho = -v_0\rho_0\nabla\cdot\delta\mathbf{p}, \tag{1.17}$$

$$(\partial_t + \lambda_1 p_0 \partial_x)\delta\mathbf{p} = -2|\alpha_0|\hat{\mathbf{x}}\delta p + a\mathbf{p}_0\delta\rho + \lambda_2\mathbf{p}_0(\nabla\cdot\delta\mathbf{p}) - (v_1/\rho_0)\nabla\delta\rho + \lambda_3 p_0\nabla\delta\mathbf{p} + \kappa\nabla^2\delta\mathbf{p} + \mathbf{f} \tag{1.18}$$

where $a = -(\alpha^{'} + \beta^{'} p_0^2) = \alpha\beta^{'}/\beta - \alpha^{'} > 0$ and $\alpha^{'} \equiv (\partial_\rho \alpha)_{\rho=\rho_0}$. Writing the equations (1.17) and (1.18) in term of a vector with elements $\phi = \{\delta\rho, \delta p, \delta n\}$ and write them in matrix form we have,

$$\partial_t \phi_{\mathbf{q}}(t) = \mathbf{M}(\mathbf{q})\cdot\phi_{\mathbf{q}}(t) + \mathbf{F}_{\mathbf{q}}(t), \tag{1.19}$$

where $\mathbf{M}$ is a matrix given by,

$$\mathbf{M}(\mathbf{q}) = \begin{bmatrix} -iq_x v_0 p_0 & -iq_x v_0\rho_0 & -iq_y v_0\rho_0 p_0 \\ ap_0 - iq_x v_1/\rho_0 & -2|\alpha_0| - iq_x\bar{\lambda}p_0 - \kappa q^2 & iq_y\lambda_2 p_0^2 \\ -iq_y v_1/(\rho_0 p_0) & iq_y\lambda_3 p_0 & -iq_x\lambda_1 p_0 - \kappa q^2 \end{bmatrix} \tag{1.20}$$

Here $\bar{\lambda} = \lambda_1 - \lambda_2 - \lambda_3$ and controls the instabilities in the ordered phase. Also, for the collection of self propelled particles $\bar{\lambda} > 0$ [Baskaran & Marchetti (2008); Bertin et al. (2006, 2009)]. Finally, the noise vector $\mathbf{F}_{\mathbf{q}}(t)$ has the components $\mathbf{F}_{\mathbf{q}}(t) = \{0, f_{\mathbf{q}}^L(t), f_{\mathbf{q}}^T(t)$, with $f_{\mathbf{q}}^L(t) = \hat{\mathbf{q}}\cdot\mathbf{f}_{\mathbf{q}}(t)$, $f_{\mathbf{q}}^T(t) = \mathbf{f}_{\mathbf{q}}(t) - \hat{\mathbf{q}}f_{\mathbf{q}}^L(t)$, and $\hat{\mathbf{q}} = \mathbf{q}/q$. The dispersion relations of the hydrodynamic modes are the eigenvalues of the matrix $\mathbf{M}(\mathbf{q})$ [Bertin et al. (2009); Mishra et al. (2010)].

Giant Density Fluctuations: In the deep ordered state, far away from the disorder-order transition point, the equations for the fluctuation in the density and the polar directions are given by,

$$(\partial_t + v_0 p_0 \partial_x)\delta\rho = -v_0\rho_0\partial_y\delta n + D\nabla^2\delta\rho + \nabla\cdot\mathbf{f}_\rho, \tag{1.21}$$

$$(\partial_t + \lambda_1\partial_x)\delta n = -v_1\partial_y(\tfrac{\delta\rho}{\rho_0}) + \kappa\nabla^2\delta n + f_y, \tag{1.22}$$

where D is a diffusion constant and $\mathbf{f}_\rho$ and f_y describe the Gaussian white noise. The hydrodynamic modes can be obtained from the equations (1.21) and (1.22) represents a sound-like waves with dispersion relation given by,

$$\omega^s_\pm = qc_\pm(\theta) - iq^2\mathscr{K}_\pm(\theta) + \mathscr{O}(q^3), \tag{1.23}$$

with $c_\pm(\theta)$ and $\mathscr{K}_\pm(\theta)$ as speed dampings that depends only on the angle θ between $\mathbf{q}$ and $\hat{\mathbf{x}}$ direction of the broken symmetry [Toner et al. (2005)]. Further, using the linearised equations we can also calculate the correlation function which can provide the static structure factor [$S(\mathbf{q})$] as follow,

$$S(\mathbf{q}) = \tfrac{1}{\rho_0 V}\langle\delta\rho_{\mathbf{q}}(t)\delta\rho_{-\mathbf{q}}(t)\rangle = \textstyle\int_{-\infty}^{\infty}\frac{d\omega}{2\pi}S(\mathbf{q},\omega), \tag{1.24}$$

where,

$$S(\mathbf{q},\omega) = \frac{1}{\rho_0 V}\int_0^\infty dt e^{i\omega t}\langle \delta\rho_{\mathbf{q}}(t)\delta\rho_{-\mathbf{q}}(t)\rangle \tag{1.25}$$

is the dynamic structure factor obtained using equations (1.21) and (1.22). Further for zero noise in the density i.e. $\mathbf{f}_\rho$, after integrating equation (1.24), we get

$$S(\mathbf{q}) = \frac{v_0^2\rho_0\Delta sin^2\theta}{(v_0+\lambda_1)^2 cos^2\theta + 4v_0v_1 sin^2\theta} \times [\frac{1}{\mathscr{K}_+(\theta)} + \frac{1}{\mathscr{K}_-(\theta)}]\frac{1}{q^2} \tag{1.26}$$

For $\theta = 0$, the singularity due to the $\frac{1}{q^2}$ term vanishes. The dependence of dynamics structure factor on $\frac{1}{q^2}$ is a robust property of uniaxial active systems and it is valid for both the polar and the nematic systems. Further, it follows the orientational order that forms a sufficiently dense collection of SPPs with anisotropic shape [Aditi Simha & Ramaswamy (2002); Ramaswamy et al. (2003); Simha & Ramaswamy (2002); Toner & Tu (1995, 1998); Toner et al. (2005)]. Also, $\frac{1}{q^2}$ do not depends on the dimensionality of the system, however other prefectors n eq. (1.26) do depends on the dimensionality of the system. In the limit of vanishing wavevector, $S(\mathbf{q})$ is the measure of the number fluctuation with,

$$\lim_{q\to 0} S(q) = \frac{\Delta N^2}{\langle N\rangle}, \tag{1.27}$$

where N and $\langle N\rangle$ are the instantaneous and average number of the particles in a region of size V, respectively, and $\Delta N^2 = \langle (N - \langle N\rangle)^2\rangle$ is the variance of number fluctuations. In an

equilibrium system $\Delta N \sim \langle N \rangle^{-1/2}$ therefore, $\frac{\Delta N}{\langle N \rangle} \sim \langle N \rangle^{1/2} \to 0$ as $\langle N \rangle \to \infty$ provided system is away from the critical point. But in the present case, due to $\frac{1}{q^2}$ term, divergence of $S(q)$ for $q \to 0$ predicted by eq. (1.26) implies that ΔN grows faster than $\langle N \rangle^{1/2}$. To understand let us rewrite eq. (1.27) as $\Delta N = \sqrt{\langle N \rangle S(q \to 0)}$. Further let us assume that the smallest accessible wave vector is of the order of the the inverse of the system size $V^{-1/d}$, with d as the dimension of the space, we have, $S(q \to 0) \sim V^{2/d} \sim \langle N \rangle^{2/d}$. This provides us, using eq. (1.27), $\Delta N \simeq \sqrt{\langle N \rangle^{\frac{2+d}{d}}}$. For $d = 2$, we get $\Delta N \simeq \langle N \rangle$.

1.6 Systems with nematic interactions on a substrate : Active nematics

Nematic interaction can be present in polar as well as in apolar particles. Here we discuss the isotropic and ordered state for apolar particles. Apolar particles interact via nematic interaction only, and the measure of the ordered phase is defined by the nematic order parameter $\mathscr{Q}$. We consider a collection of elongated active particles labeled by n, with position $\mathbf{r}_n(t)$ and the orientation described by unit vector $\hat{\nu}_n(t)$, as discussed in the previous section. A system with nematic order is defined in terms of the slow variables, density $\rho(\mathbf{r},t)$ and the nematic orientational order parameter, which is a traceless symmetric tensor $\mathscr{Q}(\mathbf{r},t)$ with components,

$$\mathscr{Q}_{\alpha\beta}(\mathbf{r},t) = \frac{1}{\rho(\mathbf{r},t)} \sum_n [\hat{\nu}_{n\alpha}(t)\hat{\nu}_{n\beta}(t) - \frac{1}{d}\delta_{\alpha\beta}]\delta(\mathbf{r} - \mathbf{r}_n(t)), \tag{1.28}$$

which the measures of the local degree of mutual alignment of the elongated axes of particles. Neglecting the effect of fluid flow and inertia, the dynamics of the orientational order is given by,

$$\partial_t \mathscr{Q} = -\frac{1}{\gamma_{\mathscr{Q}}} \frac{\delta F_{\mathscr{Q}}}{\delta \mathscr{Q}} + \mathbf{f}_{\mathscr{Q}} \tag{1.29}$$

All the terms in the above equation are traceless and symmetric. Eq. (1.29) describes the balance between the frictional torque governed by a rotational viscosity $\gamma_{\mathscr{Q}}$ and the thermodynamic torques from a free energy functional,

$$F_{\mathscr{Q}} = \int_{\mathbf{r}} [\frac{\alpha_{\mathscr{Q}}(\rho)}{2} \mathscr{Q} : \mathscr{Q} + \frac{\beta_{\mathscr{Q}}}{4} (\mathscr{Q} : \mathscr{Q})^2 + \frac{\kappa_{\mathscr{Q}}}{2} (\nabla \mathscr{Q})^2 + C_{\mathscr{Q}} \mathscr{Q} : \nabla\nabla \frac{\delta\rho}{\rho_0} + \frac{A}{2} (\frac{\delta\rho}{\rho_0})^2] \tag{1.30}$$

where, for $\alpha_{\mathscr{Q}} < 0$ and $\beta_{\mathscr{Q}} > 0$, system coarsen towards an ordered state. The third term on the right hand side of equation represents the Frank elastic energy [Chaikin & Lubensky (1995); de Gennes & Prost (1993)] and the variation in $\mathscr{Q}$ is due to elastic stresses, forth and the fifth terms represents the coupling of $\mathscr{Q}$ with ρ and the energy due to the compression with compression modulus A. Further, $\mathbf{f}_{\mathscr{Q}}$ is the tensorial white noise take care of fluctuation originated due to the activity and temperature in the system.

The equation for the density evolution is given by,

$$\partial_t \rho = -\nabla \cdot \mathbf{J}, \tag{1.31}$$

where

$$\mathbf{J} = -\frac{1}{\gamma_\rho}\nabla\frac{\delta F_{\mathscr{Q}}}{\delta\rho} + \mathbf{J}_a \tag{1.32}$$

The terms in in the right hand side of eq. (1.32) are the passive contribution with mobility γ_ρ^{-1} and the active contribution $\mathbf{J}_a$ to the total current $\mathbf{J}$ [Ramaswamy et al. (2003)]. The active current in the apolar system has the form,

$$\mathbf{J}_a = \xi_{\mathscr{Q}}\nabla\cdot\mathscr{Q} \tag{1.33}$$

also called as the active curvature current [Marchetti et al. (2013); Ramaswamy et al. (2003)]. This is the term which is responsible for the nonequilibrium nature of the system. $\xi_{\mathscr{Q}}$ controlls the strength of activity in the system. The experimental realization of curvature induced active current have been studied in detail in [Narayan et al. (2007)]. Further, the term $\xi_{\mathscr{Q}}$ is also responsible for the giant number fluctuation in an active nematics [Ramaswamy et al. (2003)].

Using the Eqs. (1.32) and (1.33), Eq. (1.31) becomes,

$$\partial_t\rho = D\nabla^2\rho + B\mathscr{Q}:\nabla\nabla\rho + \xi_{\mathscr{Q}}\nabla\nabla:\mathscr{Q} + \nabla\cdot\mathbf{f}_\rho, \tag{1.34}$$

where, $D = A/\rho_0^2\gamma_\rho$, $B = C_{\mathscr{Q}}/\rho_0\gamma_\rho$. Here, $\xi_{\mathscr{Q}}$ is taken as constant and $\mathbf{f}_\rho$ is statistically isotropic and delta correlated in space and time. In two dimensions $\mathscr{Q}$ has two independent components $\mathscr{Q}_{xx} = -\mathscr{Q}_{yy} = Scos2\theta$, $\mathscr{Q}_{xy} = \mathscr{Q}_{yx} = Ssin2\theta$. System forms uniform nematic

order for $\alpha_{\mathscr{Q}} < 0,\ \beta_{\mathscr{Q}} > 0$ in eq. (1.30). To the linear order, and the fluctuation in ρ and θ from their mean ρ_0 and $\theta = 0$, we can write, $\rho = \rho_0 + \delta\rho(\mathbf{r},t)$, $\mathscr{Q}_{ij} = diag(S,-S) + \delta\mathscr{Q}$, where $\delta\mathscr{Q}_{xy} = \delta\mathscr{Q}_{yx} \simeq 2S\theta$ and $\delta\mathscr{Q}_{xx} = -\delta\mathscr{Q}_{yy} = \mathscr{O}(\theta^2)$. Using these relations, one can calculate the space-time Fourier transforms $\delta\rho_{\mathbf{q}\omega},\ \theta_{\mathbf{q}\omega}$ and the correlation functions $S^{\rho}_{\mathbf{q}\omega} = \frac{1}{\rho_0 V}\langle|\delta\rho_{\mathbf{q}\omega}|^2\rangle$, $S^{\theta}_{\mathbf{q}\omega} = \frac{1}{V}\langle|\theta_{\mathbf{q}\omega}|^2\rangle$ and $S^{\rho\theta}_{\mathbf{q}\omega} = \frac{1}{V}\langle\delta\rho_{\mathbf{q}\omega}\theta^*_{\mathbf{q}\omega}\rangle$ [Marchetti et al. (2013); Ramaswamy et al. (2003)].

In the nematic order $\theta_{\mathbf{q}}$ has equal time correlation $S^{\theta}_{\mathbf{q}} = \int (d\omega/2\pi) S^{\theta}_{\mathbf{q}\omega} \propto 1/q^2$ and a lifetime $\propto 1/q^2$. Whereas, $S^{\rho}_{\mathbf{q}} \sim q_x^2 q_y^2/q^6$ [Ramaswamy et al. (2003)] or of the order of $1/q^2$ as for the polar flock.

1.7 Domain growth and the length scale

When quenched from disordered to the ordered state, the ordering in active nematics happen through the formation of ordered domains. The size of the ordered domain grows with time as $L(t) \sim (\frac{t}{\log t})^{1/2}$. It is the same as the equilibrium xymodel or $\mathscr{O}(2)$ model with continuous symmetry [Bray (1994)]. Starting from a random isotropic configuration for orientation and almost homogeneous density, both density and nematic order parameters coarsen with time with dynamic growth exponent $z = 2$. In the noise-free system, boundaries of the ordered-disordered domains or the interfaces are well defined. The interface's morphology is measured by calculating the cusp's exponent obtained from the small scaled-distance behavior of the two-point correlation function or large scaled-wave-vector feature of the structure factor. For smooth interface, the cusp exponent is equal to the dimension of the system (Porod's law) [Bray (1994); Oono & Puri (1988)]. Whereas in the presence of noise and other fluctuations, the morphology of the interface can change, and one can find a lower cusp exponent for diffusive interface [Das & Barma (2000)].

In this thesis, we provides a detailed description of hydrodynamic equations of motion to study dry and wet active nematics with the quenched inhomogeneity/disorder in the background environment in **chapter 2** and **chapter 3**, and the intrinsic inhomogeneity in the size of the active objects in **chapter 4**.

1.8 Active matter with inhomogeneity

Inhomogeneity is present in almost all natural systems. In the active matter also, inhomogeneity plays a crucial role in achieving a homogeneous ordered state. It can affect in both ways, positive as well as negative. Based on the nature of the inhomogeneity, it can be extrinsic or intrinsic. Extrinsic inhomogeneity can arise due to foreign objects (or obstacles) or some external fields in the system. In contrast, the intrinsic inhomogeneity appears in the form of diversity in the active objects' size or different self-propulsion speeds. Recent studies [Chepizhko et al. (2013); Das et al. (2017); Dombrowski et al. (2004); Morin et al. (2016); Reichhardt & Reichhardt (2016); Sanchez et al. (2012); Sumino et al. (2012)] addresses the impact of extrinsic inhomogeneities, on the dynamics and the steady states of a collection of active particles. The extrinsic inhomogeneity can delay the ordering kinetics and change the properties of the scaling function [Das et al. (2018b)]. Also, special kinds of inhomogeneities can lead to fast information transfer, and enhanced ordering in the flock [Chepizhko et al. (2013); Das et al. (2020a)]. These studies mainly focus on the impact of extrinsic inhomogeneity in a polar flock. Whereas, in chapter 2 and chapter 3, we address the effect of quenched inhomogeneity in dry active nematics [Kumar & Mishra (2020)] and wet active nematics, respectively. Further, intrinsic inhomogeneity in active Brownian particles system can also be interesting to study. Many studies have observed that intrinsic inhomogeneity in speed and interaction strength can accelerate the information transfer in the flock [Pattanayak et al.

(2020); Singh et al. (2021)]. Intrinsic inhomogeneity can also appear as the polydispersity in size among the active objects, e.g., the flock of *volvox barberi* have colonies of different size [Balasubramanian & McCourt (2021)] . In [Cho et al. (2012); Henkes et al. (2011)], authors study the different phases in the active Brownian system with some polydispersity in the size of the particles and the obstacles. In chapter 4 and [Kumar et al. (2021)], we study the effect of polydispersity in the dynamics of active Brownian particles.

1.9 The Lorentz lattice gas

To understand the phenomenology of the Lorentz lattice gas, let's consider a class of dynamical systems that model the motion of an object (electron, ant, a ray of light, Turing read/write head) on a simple undirected infinite lattice L. At each time step, the object hops along with the lattice from one site to another based on some deterministic rules. Let every "site" of the lattice $S \in L$ have some quenched property (R) to dictate the next step of the object on the lattice. Then the rule for the hopping of the object (or particle) is decided by the rule $S_{in}(R) \rightarrow S_{out}(R)$. R can be a mirror, rotator, or scatterer with some fixed interaction rule with the particle. This type of system is referred to as the Lorentz lattice gas or LLG [Cohen & Wang (1995a); Langton (1986)]. LLG are simple microscopic rule-based models to address several physical problems and hence gains a lot of interest in recent years.

The LLG models are not purely deterministic or probabilistic, but they can have mixed properties. Still, it successfully describes the dynamic evolution. The LLG model has pure mathematical description; still, it can address any problem in the field of computational fluid dynamics [Boghosian (1999); Lallemand (1998)], biochemistry and artificial life [Langton (1986)], graph theory [Gajardo A. (2001); Gajardo et al. (2002)], and theoretical computer science [Bowden (1998); Dewdney (1989); Langton (1986)]. Potential applications of LLG

can be to understand the order-disorder or solid-liquid interface [Meng & Cohen (1994)] and studying the dynamics of the aggregates, such as insect colonies [Langton (1986)]. Frisch et al. [Frisch et al. (1986)] and Wolfram [Wolfram (1986)] have introduced the isotropic lattice gas version of the famous Navior Stokes equation. Their models and derivatives have successfully described an effective simulation method to study complex fluids such as microemulsions [Boghosian & Coveney (2000); Boghosian et al. (1996)]. Some of the LLG models also simulate the Turning machine's dynamics and are helpful in the universal computation [Dewdney (1989)]. Further, the LLG models can be helpful to study a fundamental physical phenomenon called $diffusion$ using single particles dynamics, which is the aim of this thesis.

A classical LLG model is described by a particle moving in a Euclidean space $\mathscr{R}^d$ scattered elastically via randomly placed spheres. The classical LLG model is used to understand the dynamics of an electron in metal to understand the metal conductivity [Lorentz (1905)]. A simplified model was developed by P. Ehernfest and known as Ehrenfest's "wind tree" model [Ehrenfest & Klein (1959)]. In the Ehernfest's model, the moving electron is elastically scattered by the randomly placed diamonds whose diagonals are parallel to the coordinate axes. The above two models are considered the simplest model to study the diffusion of a particle in a random environment. A rigorous analysis of these models are complicated. The time irreversible macroscopic dynamics (diffusion) in Lorentz gas can be derived from the time-reversible microscopic dynamics only if the system or the lattice is periodic, i.e., the configuration of the scatterers repeats after a fixed interval of lattice sites [Bunimovich & Sinai (1981); Bunimovich et al. (1991); Chernov (1994)].

The classical LLG is not as simple as expected. LLG cellular automata are one of them, where the particle moves along an array of randomly distributed scatterers. Further, one of

Model	**Condition**	**Particle's dynamics**
Static Mirror	$C = 1$ or $C < 1$	anomalous super diffusion
Static rotator	$C = 1$ or $C < 1$	Closed orbit
Flipping mirror	$C = 1$	normal diffusion
Flipping rotator	$C = 1$	normal diffusion

Table 1.1 Different cases in a two dimensional Lotentz lattice gas model. $C = C_L + C_R$, where, C_L and C_L are the left and right rotators respectively.

the most general forms of the LLG model is introduced in [Bunimovich (1996)], where the scatterers can evolve with time arbitrarily.

Types of LLG

The LLG can be further divided into some subcategories. The most common models are LLG with *fixed scatterers* or static LLG (SLLG) where the environment of the scatterers do not change with the time, and the second is the LLG with *flipping scatterers* (FLLG) where the scatterer's environment can change after the interaction with a particle. In the latter case, the scatterers keep changing as time progresses. Both SLLG and FLLG describe the deterministic motion of a particle in an environment with randomly distributed scatterers. One can call the whole system as *detrminstic walk in a random environment*. Other types of LLG models involve various degrees of randomness in the scattering rules [Bezuidenhout (1999); Bunimovich & Troubetzkoy (1992); Ernst & van Velzen (1989a)].

Dynamics of a particles in LLG

The problem of bond percolation can be models using the static mirror (SM) model of LLG on a two dimensional lattice, also the problem of hull percolation where the random tilling happens in a plane with the Truchet tiles [Duplantier (1988); Pickover (1989, 1991); Roux & Sornette (1988); Smith & Boucher (1987)]. Also, the SM of LLG was related to problems like the formation of polymers and smart kinetic walks described in [Bradley (1989); Manna & Guttmann (1989); Ziff et al. (1991)]. In contrast, the flipping models of LLG were introduced

in [Bunimovich & Troubetzkoy (1993); Ruijgrok & Cohen (1988)]. The mirrors/rotators can flip their nature of interaction with a particle in the case of FLLG. Other examples of the flipping models are the industrious ant model in biochemistry [Langton (1986)] and the termites model in theoretical computer science [Dewdney (1989)]. Apart from the square lattice, the SLLG and FLLG were also introduced for triangular [Bunimovich et al. (1991); Kong & Cohen (1989)] and hexagonal lattice [Wang & Cohen (1995)] and quasi-lattice in [Wang & Cohen (1996)]. The mathematical results of LLG models explain the properties of the unbounded orbits. In contrast, the numerical results can explain the diffusion or diffusive properties of a particle in a random environment.

Bunimovich and Troubetzkoy studied both the static and flipping LLG on the regular square and triangular lattices [Bunimovich & Troubetzkoy (1992)]. They proved several theorems about the boundedness of orbits in those models [Bunimovich & Troubetzkoy (1992)] and their topological properties [Bunimovich & Troubetzkoy (1993)]. They also showed that it is possible to solve the inverse problem in some cases, i.e., determine the configuration of scatterers on the lattice from the topology of the particle trajectories [Bunimovich & Troubetzkoy (1994)]. One thing is still unclear that in what case the trajectory is closed or open or the probability of a trajectory to be open or closed—this problem we address in our work [Sampat et al. (2020)]. However, in [Cohen & Wang (1995a)], E.G.D. Cohen has performed simulation and found that all the trajectory eventually closes. This result we also find in our work on the deterministic LLG model on a square lattice [Sampat et al. (2020)]. The diffusion behavior in LLG with a variety of scattering rules has been studied numerically by E.G.D. Cohen in collaboration with T. W. Ruijgrok [Ruijgrok & Cohen (1988)], X. P. Kong [Kong & Cohen (1989, 1991a); Kong & Cohen (1991b); Ziff et al. (1991)] and F. Wang [Cohen & Wang (1995a); Cohen & Wang (1995b); Wang & Cohen (1995, 1996)]. From these works, it has been experienced that the particles show different types of diffusion, i.e., normal

diffusion or anomalous diffusion, depending upon the concentration of scatterers in the LLG. Precisely, in what proportion the left and the right rotator are present in the system. Also, the vacancies on the lattice affect the probability of the particle being in an open or closed orbit. The probabilistic flipping nature can also lead to many interesting properties, which we address in our work of one dimensional LLG [Kumar & Mishra (2019)]. Generally, we can tune the flipping probability and the concentration of scatterers as the system parameters. For a different set of parameters, single particles mean squared displacement (MSD) grows linearly with time, but the position distribution function does not seem to be Gaussian. Therefore we call such dynamics "anomalous" diffusion. Whereas for some cases, the system doesn't show diffusion; instead, it gets trapped in a closed orbit for an infinite time, as observed in our work [Kumar & Mishra (2019)]. For some critical values of system parameters, the particles show very slow dynamics (sub-diffusion) for a very long time, but it gets out of it and starts diffusing asymptotically. In addition, super-diffusion has been observed in the non-fully occupied SM model on a two dimensional lattice for all concentrations of scatterers. The normal diffusive behavior, however, was observed in the flipping models. It is to be noted that, with the LLG models with purely probabilistic scattering rules where the diffusion is always normal (see, e.g. [Ernst & van Velzen (1989a); Ernst & van Velzen (1989b); Kumar & Mishra (2019)]. Table 1.1 lists some of the results for SLLG and FLLG on different lattices based on the studies in [Bunimovich & Troubetzkoy (1992); Cohen & Wang (1995a); Grosfils et al. (1999); Kong & Cohen (1989); Ruijgrok & Cohen (1988); Ziff et al. (1991)]. A trajectory of an LLG model which visits only a finite number of vertices is always periodic [Bunimovich & Khlabystova (2002)].

Scatterers environment in LLG

With the different configurations of scatterers, i.e., left and right rotator, the LLG can be divided into three different categories: completely random (CR), random periodic (RP),

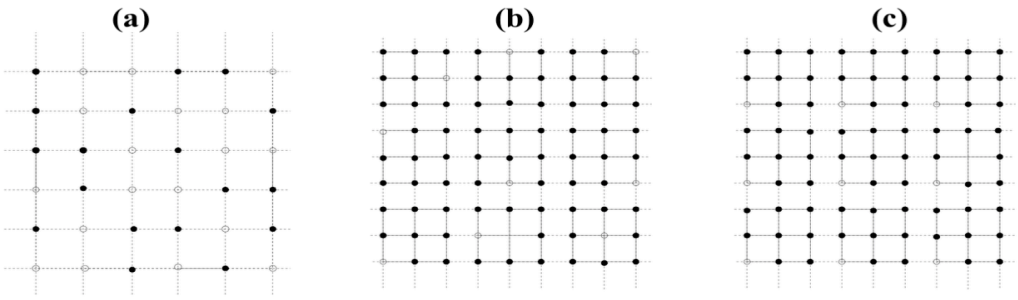

Fig. 1.2 Examples of the three types of configurations considered in [Mishra et al. (2016)] are shown. In (a) a completely random configuration is shown in which $r \simeq 1$. In (b) and (c), the entire lattice is divided in periodic blocks of size $l \times l$, where $l = 3$. The configuration in (b) is randomly periodic (RP) in that each block contains a single scatterer that is assigned to be a left rotator (open circle). The configuration in (c) is a completely periodic (CP) configuration, where the single left rotator in the same relative position in each block. In both (b) and (c) the initial ratio of rotators is $r = 1/(l \times l - 1) = 1/8$.

and completely periodic (CP) as detailed in [Mishra et al. (2016)]. The first is a completely random (CR) configuration in which the orientation of each rotator is chosen independently of the others, with the probability $(r+1)^{-1} \in [1/2, 1]$ of being a right rotator. When, $r = C_L/C_R$, the ratio of left to right scatterers, where C_L is the concentration of left rotators and C_R is the concentration of right rotators on the lattice. An example of a C_R configuration is shown in fig. 1.2(a) with ratio $r \simeq 1$. In the random-periodic configuration, we first divide the lattice into periodic $l \times l$ blocks. In each block, each rotator initially is a right rotator, then randomly select $n \leq l^2$ rotators from each block and change their orientation to become left rotators. The resulting configuration of rotators is what we refer to as a random periodic (RP) configuration. Further, as $l \to \infty$, a random-periodic configuration becomes a completely random configuration. An example of a RP configuration is shown in fig. 1.2(b). In the third type of configuration we consider, we choose a single $l \times l$ block, again containing a single left rotator, which we periodically place over the entire lattice. The result is what we refer to as a completely periodic (CP) configuration. An example of a CP configuration is shown in fig. 1.2(c).

We provide a detailed description of the static and flipping cases of the Lorentz lattice gas model in one and two dimensions, and the motion of a particle in it in **chapter 5** and **chapter 6**.

1.10 Summary of the coming chapters

In the coming chapters, we discuss our work and results in detail.
First, we discuss the effect of quenched field disorder on the ordering kinetics and steady-state of collection of the active apolar particles with nematic order (active nematics). We model a system of apolar particles, generally termed active nematics, with field disorder quenched in time and space. The model is studied using coarse-grained hydrodynamic equations of motion for slow variables. There are two different scenarios; in one case, we consider the system without momentum conservation, i.e., the "dry" system. In another case, we consider the momentum conservation where the system is suspended in a fluid, i.e., the "wet" system. Both the cases are studied separately. In the case of dry active nematics, the numerical solution of equations of motion and the calculation of two-point orientation correlation function using linear approximation show that the ordered steady-state follows a disorder-dependent crossover from quasi-long-range order to short-range order. Such crossover is due to the pinning of $\pm 1/2$ topological defects in the presence of finite disorder, which breaks the system in uncorrelated domains. Whereas in the case of wet active nematics, we find that the disorder slows the ordering kinetics. Further, we observe that the density growth was found to be faster than the nematic order parameter, which is not seen for the dry case. Further, the system shows dynamics scaling in the presence of disorder but no static scaling.

Next, we study the effect of polydispersity in the size of active Brownian particles (ABPs) on their dynamic and steady-state. We find that the polydispersity enhances the dynamics

of ABPs and the effective diffusion coefficient increases on increasing the polydispersity. We find four distinct phases of particles dynamics, solid jammed and liquid jammed phases, MIPS-liquid phase, and pure liquid phase with enhanced diffusivity.

Finally, we investigate the dynamics of a particle in a Lorentz lattice gas where a particle moves with some fixed rule along with the bonds of a one or two dimensional lattice. Lattice is decorated with different rotators (left/right or transmitters/reflectors) or obstacles either periodically or randomly. The first problem is a probabilistic model of the one-dimensional Lorentz lattice gas, where the rotators can interchange their nature of the interaction, with a particle, with some probability. In this case, we find that the particles show three phases asymptotically: ballistic motion, anomalous diffusion, and confinement for the chosen sets of system parameters. The second problem is a deterministic model of the two-dimensional Lorentz lattice gas, where the rotators do not change their nature. Still, there are some vacant sites in the lattice where the direction of particle motion remains unaffected. We perceive that the particle show two phases of its motion: the first phase is characterized by anomalous diffusion and a power-law decay of the probability of being in an open trajectory. The second phase is characterized by sub-diffusive motion and exponential decay of the probability of being in an open trajectory.